Performance Enhancement of SWIPT by Utilizing the Distance Dependent Bandwidth of Underwater Channel for Cooperative NOMA based UASNs

Deepa R., *Graduate Student Member, IEEE*, V. P. Harigovindan, *Senior Member, IEEE*, and Veerapu Goutham, *Member, IEEE*

***Abstract*—Underwater acoustic sensor networks (UASNs) support a variety of oceanic applications but suffer from limited communication bandwidth, reliability, and energy efficiency. Cooperative non-orthogonal multiple access (CNOMA) with simultaneous wireless information and power transfer (SWIPT) schemes are proposed for UASNs to meet these constraints. The unique characteristic of underwater acoustic channels compared to terrestrial wireless channels is the distance-dependent bandwidth, which provides additional bandwidth to the near user compared to the far user in NOMA-based UASNs. In this research work, we propose to enhance the performance of power splitting (PS) and time switching (TS) SWIPT schemes by utilizing this additional bandwidth at the near user in NOMA-based UASNs. We consider a CNOMA-based UASN and derive closed-form expressions for average achievable rates, energy efficiency, and outage probability with improved PS-SWIPT and TS-SWIPT schemes. From the analytical results, it is evident that the average achievable rate, energy efficiency and outage probability performances are significantly improved with the proposed methods. The analytical results are corroborated with extensive simulation studies.**

Link to graphical and video abstracts, and to code: https://latamt.ieeer9.org/index.php/transactions/article/view/9685

***Index Terms*—Average achievable rate, Energy efficiency, Non-orthogonal multiple access, Outage probability, Simultaneous wireless information and power transfer, Underwater acoustic sensor networks.**

I. Introduction

UNDERWATER wireless sensor networks (UWSNs) are increasingly utilized in oceanic applications such as military surveillance, ocean exploration, underwater multimedia, assisted navigation, pollution management, etc. These networks comprise of wirelessly connected autonomous underwater vehicles (AUVs), buoys, and multiple sensor nodes that are strategically placed in critical region of ocean. Wireless communications among these network components can be achieved by using optical, acoustic, or radio frequency (RF) signals. Although RF signals offer greater bandwidth, they suffer significant absorption losses in underwater conditions. Similarly, optical wireless communications face challenges including dispersion from underwater particles, absorption losses, and interference from ambient light, limiting them to shorter ranges. As a result, UWSNs primarily rely on acoustic signals due to their ability to support long-distance communications [1]. Despite of its advantages, acoustic signals in underwater communications are constrained by bandwidth limitations, high transmission loss, multipath effects, long propagation delays, and Doppler spread. The available bandwidth in UASNs are limited to maximum of 100 kHz, which is significantly lower than terrestrial wireless sensor networks (WSNs) [2]. This results in lower throughput and transmission rates for UASNs compared to WSNs [3]. Recently, NOMA is considered to be an effective candidate to improve the achievable data rates in terrestrial WSNs. In order to achieve higher data rates within the constrained communication bandwidth, NOMA is also viewed as a potential approach for the next generation UASNs. Authors in [4], [5], [6] proposed NOMA for UASNs to enhance achievable data rate. Either the power domain or the code domain can be used to implement NOMA. In the power-domain NOMA, the transmitting node can simultaneously send multiple users information in a single resource block by splitting the transmission power among the users based on their distance from the base station. The principle of NOMA is based on superposition coding and successive interference cancellation (SIC) techniques [7]. CNOMA is a technique that enables users with better channel conditions to decode and forward information for users with weaker channels, thus acting as relays in a cooperative transmission strategy [8], [9]. This approach improves reliability and spectral efficiency, particularly in challenging environments such as UASNs, where channel conditions can fluctuate greatly with distance. By integrating power-domain NOMA with user cooperation, CNOMA proves to be particularly effective for underwater networks where direct transmission link to distant users often suffer severe signal degradation.

In UASNs, another significant challenge is to achieve energy efficiency. AUVs and sensor nodes typically rely on batteries. However, replacing or recharging a battery in a deep underwater environment is an extremely difficult task. Therefore, an important objective for researchers is to reduce the power consumption of underwater nodes, which can improve the energy efficiency and lifetime of the nodes [4].

The associate editor coordinating the review of this manuscript and approving it for publication was Carolina Del-Valle-Soto (*Corresponding author: V. P. Harigovindan*).

R. Deepa, and V. P. Harigovindan are with the Department of Electronics and Communication Engineering, National Institute of Technology Puducherry, Karaikal, India (e-mails:ec22d1007@nitpy.ac.in, and hari@nitpy.ac.in).

V. Goutham is with the Department of Communication Engineering, School of Electronics Engineering, Vellore Institute of Technology, Vellore, Tamilnadu, India (e-mail: veerapu.goutham@vit.ac.in).

Energy harvesting techniques provide an effective solution for extending the lifespan of sensor nodes by converting ambient energy into electrical energy. In the literature, different energy harvesting strategies have been proposed for UASNs, such as piezoelectric transducer, microbial fuel cell (MFC), hybrid harvesting utilizing MFC and piezoelectric transducer, etc. Acoustic signals from the nearby nodes, AUVs, and aquatic animals are converted into electric signals by piezoelectric transducers [10]. Whereas in a microbial fuel cell, the chemical action of bacteria is used to generate electrical energy [11]. MFCs and piezoelectric transducers are both used in hybrid energy harvesting, which is an innovative method to gather energy from several sources [12]. In a galvanic cell, zinc and brass are used as electrodes in the sensor node, with seawater as an electrolyte [13]. In ocean thermal energy harvesting, energy is harvested by using the temperature difference on the surface and at some depth of the ocean [14]. The utilization of acoustic signals for energy harvesting is also known as the wireless power transfer technique (WPT). However, the acoustic signals are capable of carrying information as well as energy, which allows us to perform simultaneous WPT and wireless information transmission in UASNs. This has led to simultaneous wireless information and power transfer (SWIPT) in UASNs. SWIPT is classified as power-splitting SWIPT (PS-SWIPT) and time-switching SWIPT (TS-SWIPT). In PS-SWIPT, the received acoustic signal is divided into energy harvesting and information decoding components based on a specific power-splitting ratio [15]. Conversely, TS-SWIPT alternates between energy harvesting and information decoding modes over time [16].

The unique characteristics of the underwater acoustic channels are their distance-dependent usable bandwidth, acoustic spreading, propagation loss, and fading effects [17]. Among these, a unique feature of UASNs compared to terrestrial RF systems is the dependence of the transmission bandwidth on the transmission distance [18], [19], [20]. The bandwidth is broader for shorter communication distances and narrower for longer communication distances. As a result, the near user that is closest to the transmitter receives higher bandwidth than the other users. In this research work, we propose a novel SWIPT technique for CNOMA-based UASNs, which will make use of the additional bandwidth of the near user, achieved by the virtue of its location close to the AUV, to enhance the harvested energy. As previous works have not considered this effect, we address the gap by introducing improved PS-SWIPT and TS-SWIPT schemes that utilize this feature for enhanced system performance.

The rest of the paper is organized as follows: Section II consists of a literature survey. Section III presents the system model, which consists of a channel model of the UASNs and also presents the network scenario considered in our work. Section IV describes the proposed SWIPT schemes for CNOMA in UASNs. Section V presents results and discussions. Section VI summarizes the results and concludes the work.

II. Literature Survey

In this section, we present a detailed literature review on NOMA, energy harvesting, and SWIPT techniques for UASNs. Recently, NOMA has advanced significantly to meet the challenges of bandwidth and energy constraints of UASNs. In [4], the authors present full-duplex cooperative relaying with NOMA (FD-CR-NOMA) for UASNs for improving the channel capacity and energy efficiency. With the spatial diversity, the cooperative relaying strategy is found to be effective in improving the reliability and energy efficiency of UASNs. To provide efficient simultaneous communication for UASNs, the authors propose a hybrid NOMA-based MAC protocol (HN-MAC) in [6]. HN-MAC assigns communication resources and classifies users by combining power-domain and code-domain NOMA. In [5], the authors discuss a receiver architecture based on a deep neural network for downlink NOMA for acoustic communication in an underwater channel.Energy sources such as thermal, solar, radio frequency, wind, and mechanical vibration can be used for energy harvesting in sensor networks [21]. Studies investigate the potential of energy harvested from these sources to effectively recharge low-power electronic devices, including wireless sensor nodes, portable electronics, and communication systems. In [22], the authors analyze piezoelectric transducers, which transform acoustic signals from sources such as the base station, near node, AUV, and aquatic animals into electrical signals. In [23], authors study microbial fuel cells that generate electrical energy from the chemical reactions of bacteria. In [12], the authors present a hybrid energy harvesting method that combines microbial fuel cells with piezoelectric transducers to enhance energy capture efficiency.Furthermore, SWIPT for terrestrial networks has been proposed for maximizing the network lifetime [24], [25], [39], [27], [28]. Power-splitting relaying SWIPT (PSR-SWIPT) and time-switching relaying SWIPT (TSR-SWIPT) are the two most common types of cooperative SWIPT for terrestrial networks. In [29], the authors compare the effectiveness of full-duplex users utilizing these two different protocols, PSR and TSR, for wireless energy harvesting applications.The authors of [30] examine the impact of using the TSR protocol with NOMA for both direct and coordinated transmissions. In [25], the authors investigate the process of selecting optimal relays for multi-relay downlink CNOMA networks with SWIPT in the presence of interference. Additionally, SWIPT can be modified for relay node-based CR-NOMA communications by utilizing the TSR or PSR protocols. Recently, several studies have proposed SWIPT for UWSNs [30], [31], [32]. The authors of [30] propose a novel reinforcement learning (RL) based method to enhance throughput and WPT in acoustically enabled SWIPT systems, resulting in more sustainable UWSNs that utilize AUVs for data transfer. In order to maximize harvested energy to prolong the battery life, the authors of [31] propose time reversal TR-NOMA, which is centered on outfitting AUVs with SWIPT capability. The authors examine current methods for underwater wireless power and data transfer in [32], emphasizing developments from the last five years of research.In [33], [34], the authors discuss the channel modeling of UWSNs. The distance-dependent

bandwidth refers to the phenomenon where the bandwidth available for transmission decreases as the distance between communication nodes increases. This reduction is primarily due to signal attenuation caused by absorption and scattering in the underwater environment. In [35], the authors study the relationship between effective use of the available bandwidth, energy consumption,and transmission delay in UASNs.To the best of the authors' knowledge, this is the first research work to propose underwater-specific SWIPT schemes that utilize the distance-dependent bandwidth of underwater channels to harvest additional energy to enhance the performance of the conventional SWIPT schemes. In this manuscript, differently from the existing research works, which consider conventional terrestrial SWIPT schemes for underwater networks, we propose improved PS-SWIPT (IPS-SWIPT) and improved TS-SWIPT (ITS-SWIPT) schemes for CNOMA-based UASNs. The major contributions of this research work are as follows:

1) We propose IPS-SWIPT and ITS-SWIPT schemes for CNOMA-based UASNs, which utilize the additional bandwidth available at the near user due to the distance dependence on the bandwidth in the underwater channel to harvest additional energy.
2) We derive accurate analytical expressions for average achievable rate, energy efficiency and outage probability for the proposed IPS-SWIPT CNOMA and ITS-SWIPT CNOMA schemes by considering the underwater specific characteristics, such as distance dependent usable bandwidth, transmission power, acoustic spreading, and underwater path losses.
3) From the analytical results, it is evident that the proposed IPS-SWIPT CNOMA and ITS-SWIPT CNOMA schemes have significantly improved the average achievable rates and outage probability performance as well as energy efficiency compared to the conventional PS-SWIPT CNOMA and TS-SWIPT CNOMA schemes. Finally, the analytical results are corroborated with extensive simulation studies.

III. System Model

A. Channel Model

The power output of the underwater acoustic transmitter is represented by the source level. Underwater receivers are usually arrays of hydrophones. At the receiver, the received signal-to-noise ratio (SNR) in decibels (dB) is provided by $\delta = (SL + DI) - (TL + NL)$, where DI is the directivity index and NL is the noise level that varies with environmental factors like turbulence, marine activities, and thermal noise. Hence, SL is the source level that depends on signal intensity at a reference distance (I_{REF}), η is the power conversion efficiency, and TL is the transmission loss that accounts for absorption as well as spreading losses [30], [38]. SNR (linear scale) between any transceiving nodes is given by $\delta = \frac{P}{\psi_C \times TL \times NL}$ and $\psi_C = \frac{\psi \times I_{REF}}{\eta \times DI}$, where P is the total transmitted power and ψ is $2\pi H$ for shallow water and 4π for deep water [4]. The analysis considers underwater channels with rayleigh fading and distance-dependent bandwidth. We also consider ambient noise from turbulence, shipping, wind, as well as thermal sources.

B. Network Model

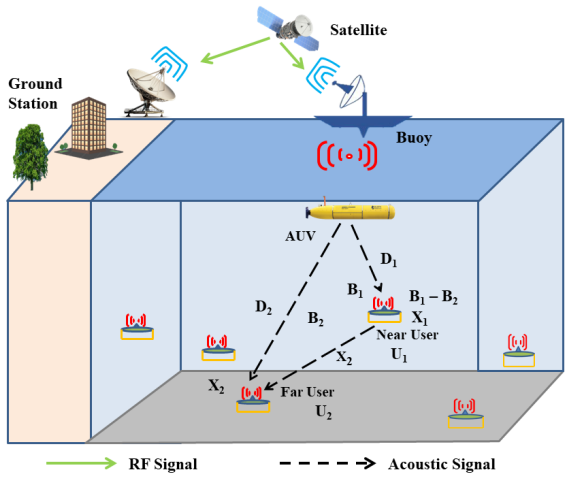

Fig. 1. SWIPT based CNOMA in UASNs.

We consider an underwater scenario that includes an AUV and two underwater sensor nodes at different locations, one of which is close to the AUV (near user) represented as U_1 and the other is the far user represented as U_2, as shown in Fig. 1. The distances between AUV and U_1 as D_1 and U_2 as D_2 where $D_1 < D_2$. The bandwidth available to U_1 and U_2 is B_1 as well as B_2, respectively, where $B_1 > B_2$. The symbol intended for U_1 is X_1 and U_2 is X_2. The distance dependence of the underwater channel leads to larger communication bandwidth to nodes located at shorter distances from the transmitter. Hence, the respective bandwidths of U_1 and U_2 are calculated by $B_1 = bD_1^{-q}, B_2 = bD_2^{-q}$ where b is the bandwidth coefficient and q is the bandwidth exponent [9]. In bandwidth B_2, AUV sends the superimposed signals X_1 and X_2 for U_1 and U_2. So additional bandwidth at the U_1 is calculated as $B_{ADD} = B_1 - B_2$. The AUV sends the acoustic signals to U_1 in additional bandwidth for energy harvesting. U_1 also serves as a relay, which first decodes the far user symbol X_2 and performs SIC to obtain its own symbol X_1. After successful decoding, U_1 sends symbol X_2 to U_2 in the next time slot by using the harvested energy.

IV. Proposed Schemes

This section presents the details of the proposed schemes: (1) Improved power splitting SWIPT CNOMA in UASNs by utilizing additional bandwidth (IPS-SWIPT CNOMA) and (2) Improved time switching SWIPT CNOMA in UASNs by utilizing additional bandwidth (ITS-SWIPT CNOMA). This section also covers the various aspects such as energy harvesting, system model, average achievable rate, outage probability, and energy efficiency of the proposed schemes.

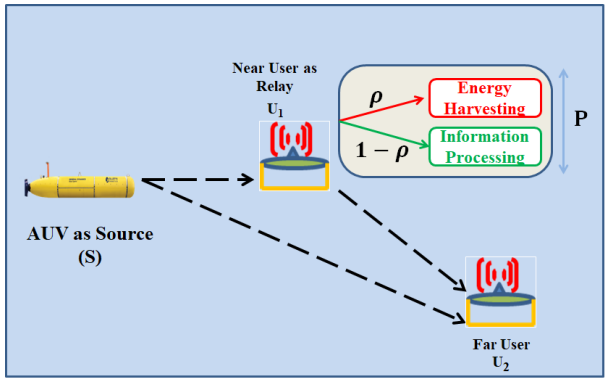

Fig. 2. Power Splitting SWIPT CNOMA for UASNs.

A. Improved Power Splitting SWIPT CNOMA in UASN by utilizing the Additional Bandwidth (IPS-SWIPT CNOMA)

1) Energy Harvesting Mechanism of IPS-SWIPT CNOMA: We consider the PS-SWIPT scheme at U_1, which operates in half-duplex mode and also acts as a relay for U_2. The system model is shown in Fig. 2. U_1 implements piezoelectric energy harvesting based on the PS-SWIPT, where the ρ portion of the received power is utilized for energy harvesting and the remaining $(1-\rho)$ portion is used for information decoding, with $0<\rho<1$ serving as the PS factor [39]. Accordingly, the energy harvested by U_1 using the PS-SWIPT scheme is given by [36]

$$P_{h(PS)} = \frac{0.7n \times 10^{\frac{\rho(SL-TL-NL)+RVS}{10}}}{4R_P} \tag{1}$$

where n is the number of hydrophones, RVS is the receiving voltage sensitivity of the hydrophone, and R_P is the load impedance of the harvesting hydrophone. The harvested energy at U_1 using additional bandwidth is given by [36]

$$P_{h(ADD)} = \frac{0.7n \times 10^{\frac{SL-TL-NL+RVS}{10}}}{4R_P} \tag{2}$$

where the signal sent in the B_{ADD} is exclusively used for energy harvesting. The total energy harvested by U_1 in the IPS-SWIPT scheme is given by

$$P_{h(IPS)} = P_{h(PS)} + P_{h(ADD)} \tag{3}$$

$P_{h(IPS)}$ value is used to calculate the average achievable rate, outage probability, and energy efficiency. The proposed schemes can be implemented with minor hardware changes, allowing the harvesting of additional energy with minimal additional processing power. This provides a positive energy balance to support energy limited UASNs.

2) System Model of IPS-SWIPT CNOMA: The superimposed signal transmitted from AUV, which consists of symbols X_1 and X_2, is given by [4]

$$X(t) = \sqrt{\alpha_1 P}X_1(t) + \sqrt{\alpha_2 P}X_2(t) \tag{4}$$

where α_1 and α_2 are the power allocation factors for the symbols X_1 and X_2, respectively, $\alpha_2 > \alpha_1$, and $\alpha_1+\alpha_2=1$. The signal received by U_1 from the AUV is given by [4]

$$Y_1(t) = \frac{h_1}{\sqrt{\psi_c T L_{1(d,f)}}}\left(\sqrt{\alpha_1 P}X_1(t) + \sqrt{\alpha_2 P}X_2(t)\right) + n_1(t) \tag{5}$$

where h_1 is the channel coefficient between the source and U_1, and $n_1(t)$ represents noise. The signal-to-interference-plus-noise ratio (SINR) for the symbols X_1 and X_2 at U_1 is given by [4]

$$\gamma_{SU_1}^{X_2} = \frac{\alpha_2(1-\rho)\delta_1|h_1|^2}{\alpha_1(1-\rho)\delta_1|h_1|^2+1}, \gamma_{SU_1}^{X_1} = \frac{\alpha_1(1-\rho)\delta_1|h_1|^2}{\zeta\alpha_2(1-\rho)\delta_1|h_1|^2+1} \tag{6}$$

where $\delta_1 = \frac{P}{\psi_c T L_{1(d,f)}\sigma_1^2(f)}$ is the SNR between AUV and U_1, ζ is the SIC inefficiency, with $\zeta=0$ being perfect SIC and $0<\zeta<1$ indicating imperfect SIC. The signal received by U_2 from the AUV is given by

$$Y_2(t) = \frac{h_2}{\sqrt{\psi_c T L_{2(d,f)}}}\left(\sqrt{\alpha_1 P}X_1(t) + \sqrt{\alpha_2 P}X_2(t)\right) + n_2(t) \tag{7}$$

where h_2 is the channel coefficient between the AUV and U_2. In the proposed IPS-SWIPT CNOMA, U_1 transmits symbol X_2 to U_2 using harvested energy in the next time slot. Hence, the received signal at U_2 from U_1 is given by

$$Y_{12}(t) = \frac{h_{12}}{\sqrt{\psi_c T L_{12(d,f)}}}\sqrt{P_{h(IPS)}}X_2(t) + n_{12}(t) \tag{8}$$

where h_{12} is the channel coefficient between U_1 and U_2. U_2 implements selection diversity to choose the symbol X_2, which is received from both the AUV and U_1, to enhance the SINR. Subsequently, the SINR for the symbol X_2 at U_2 can be obtained by

$$\gamma_{U_{12}}^{X_2} = \max\left\{\frac{\alpha_2\delta_2|h_2|^2}{\alpha_1\delta_2|h_2|^2+1}, \delta_{h(IPS)}|h_{12}|^2\right\} \tag{9}$$

where $\delta_{h(IPS)} = \frac{P_{h(IPS)}}{\psi_c T L_{12(d,f)}\sigma_{12}^2(f)}$ is the SNR between U_1 and U_2.

3) Average Achievable Rate of IPS-SWIPT CNOMA: The average achievable rate at U_1 is given by [9]

$$C_{X_{1(IPS)}} = \frac{1}{2}\int_{f_l}^{f_u} E\left[\log_2\left(1+\gamma_{SU_1}^{X_1}\right)\right] df \tag{10}$$

where f_l and f_u are the lower bound and upper bound frequencies. Let assume, $A_1 = \log_2\left(1+\gamma_{SU_1}^{X_1}\right)$. From (6), A_1 is expressed as

$$A_1 = \log_2\left(1+\frac{\alpha_1(1-\rho)\delta_1|h_1|^2}{\zeta\alpha_2(1-\rho)\delta_1|h_1|^2+1}\right) \tag{11}$$

Let U is random variables, which is denoted as, $U \triangleq \frac{\alpha_1(1-\rho)\delta_1|h_1|^2}{\zeta\alpha_2(1-\rho)\delta_1|h_1|^2+1}$, by substituting U into (11), the average achievable rate at U_1 is given by

$$C_{X_{1(IPS)}} = \frac{1}{2}\int_{f_l}^{f_u}\int_0^{\infty}\log_2\left(1+U\right)f_U(u)\,du\,df \tag{12}$$

By using $\int_0^\infty \log_2(1+U) f_U(u)du = \frac{1}{ln2}\int_0^\infty \frac{1-F_U(u)}{1+u}du$, the cumulative distribution functions (CDF) of randon variable u with the rate parameter λ_1 is given by

$$F_U(u) = \begin{cases} \left(1 - e^{-\frac{\lambda_1 \ u}{\delta_1(1-\rho)(\alpha_1 - u\zeta\alpha_2)}}\right) & \text{if } u < \frac{\alpha_1}{\zeta\alpha_2} \\ 1 & \text{if } u \geq \frac{\alpha_1}{\zeta\alpha_2} \end{cases} \quad (13)$$

The analytical expression of the average achievable rate at U_1 is obtained as

$$C_{X_{1(IPS)}} = \frac{1}{2ln2}\int_{f_l}^{f_u}\int_0^\infty \frac{(1-F_U(u))}{1+u}du \ df \quad (14)$$

The average achievable rate at the U_2 is given by

$$C_{X_{2(IPS)}} = \frac{1}{2}\int_{f_l}^{f_u} E\left[\log_2\left(1+\gamma_{U_{12}}^{X_2}\right)\right] df \quad (15)$$

Let assume $A_2 = \log_2\left\{1+\max\left(\frac{\alpha_2\delta_2|h_2|^2}{\alpha_1\delta_2|h_2|^2+1}, \delta_{h(IPS)}|h_{12}|^2\right)\right\}$ by substituting (9) in (15). Assume Y and Z are random variables, which are denoted as $Y \triangleq \frac{\alpha_1\delta_1|h_1|^2}{\alpha_2\delta_1|h_1|^2+1}$ and $Z \triangleq \left(\delta_{h(IPS)}|h_{12}|^2\right)$ and $W \triangleq max\{Y,Z\}$. The CDFs of the above random variables are given by

$$F_Y(y) = \begin{cases} \left(1 - e^{-\frac{\lambda_2 \ y}{\delta_2(\alpha_2 - z\alpha_1)}}\right) & y < \frac{\alpha_2}{\alpha_1} \\ 1 & y \geq \frac{\alpha_2}{\alpha_1} \end{cases} \quad (16)$$

$$F_Z(z) = \left(1 - e^{-\frac{\lambda_{12} \ z}{\delta_{h(IPS)}}}\right) \quad (17)$$

$$F_W(w) = \begin{cases} F_Y(y)F_Z(z) & w < \frac{\alpha_2}{\alpha_1} \\ 1 & w \geq \frac{\alpha_2}{\alpha_1} \end{cases} \quad (18)$$

where the rate parameter of Y is λ_2 and Z is λ_{12}. The analytical expression of the average achievable rate at U_2 is obtained as:

$$C_{X_{2(IPS)}} = \frac{1}{2ln2}\int_{f_l}^{f_u}\int_0^\infty \frac{(1-F_W(w))}{1+w}dwdf \quad (19)$$

The average achievable rate of IPS-SWIPT CNOMA is given by, $C_{X_{1(IPS)}} + C_{X_{2(IPS)}}$.

4) Outage Probability of IPS-SWIPT CNOMA: The outage probability is determined when the received power falls below the threshold power. Assume that the threshold levels for symbols X_1 and X_2 are R_1 and R_2. The bandwidth is divided into L narrow sub-bands, each undergoing flat fading, to simplify the outage probability analysis for frequency-selective channels [9]. The outage probability for the X_1 symbol [39] across these sub-bands is then expressed by

$$P_{X_{1(IPS)}}^{\text{out}} = \frac{1}{L}\sum_{j=1}^{L}\left[1 - \Pr\left(\gamma_{SU_1}^{X_2} > \theta_2, \gamma_{SU_1}^{X_1} > \theta_1\right)\right]$$

$$P_{X_{1(IPS)}}^{\text{out}} = \frac{1}{L}\sum_{j=1}^{L}\left[1 - \exp\left(-\left(\frac{\lambda_1\theta_2}{(1-\rho)\delta_1(\alpha_2 - \theta_2\alpha_1)} - \frac{\lambda_1\theta_1}{(1-\rho)\delta_1(\alpha_1 - \zeta\theta_1\alpha_2)}\right)\right)\right] \quad (20)$$

The outage probability for the X_2 symbol across the sub-bands is expressed as follows [39]

$$P_{X_2}^{\text{out}} = \frac{1}{L}\sum_{j=1}^{L}\left[\left\{\Pr\left(\gamma_{U_{12}}^{X_2}\right) < \theta_2\right\} \times \left\{\Pr\left(\gamma_{SU_1}^{X_2}\right) > \theta_1\right\} + \left\{\Pr\left(\gamma_{SU_1}^{X_2}\right) < \theta_2, \Pr\left(\gamma_{SU_2}^{X_2}\right) < \theta_2\right\}\right] \quad (21)$$

$$P_{X_2}^{\text{out}} = \frac{1}{L}\sum_{j=1}^{L}\left[\left\{\left(1 - e^{-\frac{\lambda_2\theta_2}{\beta_2(\alpha_2 - \theta_2\alpha_1)}}\right)\left(1 - e^{-\frac{\lambda_{12}\theta_2}{\delta_{h(IPS)}}}\right)e^{-\frac{\lambda_2\theta_2}{(1-\rho)\delta_1(\alpha_2-\theta_2\alpha_1)}}\right\} + \left\{\left(1 - e^{-\frac{\lambda_1\theta_2}{(1-\rho)\delta_1(\alpha_2-\theta_2\alpha_1)}}\right)\left(1 - e^{-\frac{\lambda_2\theta_2}{\beta_2(\alpha_2-\theta_2\alpha_1)}}\right)\right\}\right] \quad (22)$$

5) Energy Efficiency of IPS-SWIPT CNOMA: One of the key factors that determines how much energy is harvested and efficiently utilized by the sensor nodes is the energy efficiency. The energy efficiency is given by [9]

$$EE_{IPS} = \frac{(1-P_{X_1}^{out})C_{X_{1(IPS)}} + (1-P_{X_2}^{out})C_{X_{2(IPS)}}}{E_{IPS}} \quad (23)$$

where E_{IPS} is the total energy used by the sensor nodes in the IPS scheme.

B. Improved time Switching SWIPT CNOMA in UASN by utilizing the Additional Bandwidth (ITS-SWIPT CNOMA)

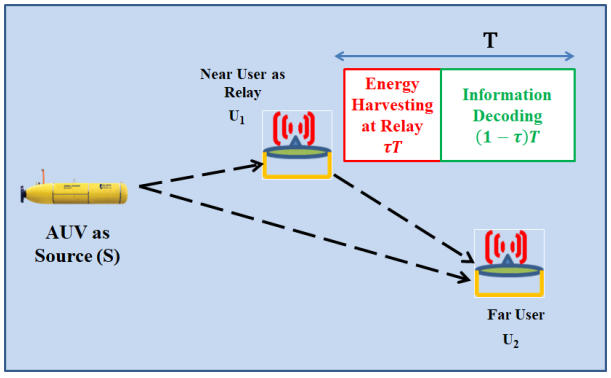

Fig. 3. Time Switching SWIPT CNOMA for UASNs.

We consider U_1 operates in half-duplex mode, implementing piezoelectric energy harvesting based on the TS-SWIPT scheme where the τ portion of the total time T is allocated for energy harvesting, and the remaining $(1-\tau)$ portion is used for information decoding, with $0 < \tau < 1$ serving as the TS factor [40] as shown in Fig. 3. Accordingly, the energy harvested by U_1 using TS-SWIPT is given by [36], [40]

$$E_{h(TS)} = \frac{0.7n\tau T \times 10^{\frac{(SL-TL-NL)+RVS}{10}}}{4R_P} \quad (24)$$

where T is the total duration of the time slot. The available transmit power at U_1 is given by [36]

$$P_{h(TS)} = \frac{0.7n2\tau 10^{\frac{(SL-TL-NL)+RVS}{10}}}{(1-\tau)4R_P} \quad (25)$$

where $((1-\tau)/2)T$ represents the effective duration for information transmission after allocating τT for energy harvesting. The total available power harvested by U_1 using TS-SWIPT scheme can be calculated by

$$P_{h_{(ITS)}} = P_{h(TS)} + P_{h(ADD)} \tag{26}$$

The signal received by the U_1 from AUV is given in (5). Based on the TS-SWIPT scheme, the SINR for the symbol X_1 and X_2 at the U_1 are given by

$$\gamma^{X_2}_{U_1(ITS)} = \frac{\alpha_2\delta_1|h_1|^2}{\alpha_1\delta_1|h_1|^2+1}, \ \gamma^{X_1}_{U_1(ITS)} = \frac{\alpha_1\delta_1|h_1|^2}{\zeta\alpha_2\delta_1|h_1|^2+1} \tag{27}$$

The signal received by U_2 from the AUV is calculated as in (7), and U_2 combines the symbol X_2 from the source and U_1 using the selection combining technique as in (9). The average achievable rate at U_2 and U_1 is calculated as in (10) and (15). The analytical expression of the average achievable rate for U_2 and U_1 are given by

$$C_{X_{2(ITS)}} = \frac{1-\tau}{2ln2}\int_{f_l}^{f_u}\int_0^{\infty}\frac{(1-F_{U'}(u))}{1+u}dudf \tag{28}$$

$$C_{X_{1(ITS)}} = \frac{1-\tau}{2ln2}\int_{f_l}^{f_u}\int_0^{\infty}\frac{(1-F_{W'}(w))}{1+w}dwdf \tag{29}$$

The average achievable rate of ITS-SWIPT CNOMA is given by $C_{X_{1(ITS)}} + C_{X_{2(ITS)}}$. The outage probabilities of X_2 and X_1 are calculated as in (20) and (21) by considering $\theta_1 = 2^{\frac{2R_1}{\Delta f_j(1-\tau)T}} - 1$ and $\theta_2 = 2^{\frac{2R_2}{\Delta f_j(1-\tau)T}} - 1$ is the threshold power for U_1 and U_2 in ITS-SWIPT CNOMA. The energy efficiency of the ITS scheme is calculated as in (23).

V. Results and Discussions

The analytical results are obtained by using the mathematical models presented in Section IV-A and IV-B. Monte Carlo simulations are performed using MATLAB 2024b. The parameters used for plotting the figures are summarized in Table I. We averaged the simulation results over 50 simulation runs. The results are plotted with 95 percent confidence interval. Fig. 4 shows the variation of average achievable rate of IPS-SWIPT CNOMA with the distance between the source and the far user. It is evident that the average achievable rate of IPS-SWIPT CNOMA decreases as the distance increases, primarily due to the dependence of the SNR on transmission distance. However, the introduction of additional bandwidth significantly improves the average achievable rate compared to the conventional PS-SWIPT CNOMA. Fig. 5 illustrates the outage probability for symbol X_1 as a function of the distance between the source and the far user. The outage probability increases with distance, but the use of IPS-SWIPT results in lower outage probabilities across all distances compared to the conventional PS-SWIPT CNOMA. Fig. 6 presents the energy efficiency of the IPS-SWIPT scheme. The energy efficiency decreases with increasing distance, consistent with the average achievable rate and outage probability trends. It can be observed from the results that the proposed IPS-SWIPT CNOMA scheme, the energy efficiency, can be substantially improved compared to the conventional PS-SWIPT CNOMA. Fig. 7 shows the variation of the average achievable rate of ITS-SWIPT CNOMA with the distance between the source and the far user. Fig. 8 illustrates that the outage probability increases with distance. But from the results, it is evident that the use of ITS-SWIPT results in lower outage probabilities

TABLE I
System Parameters

Parameter	Symbol	Value
Transmitted Power	P	10 W
Power Allocation for bit x_1	α_1	0.9
Coefficient	b	19.76 dB re kHz
Exponent	q	0.59 dB re kHz/km
Receiver voltage sensitivity	RVS	-150 dB
Threshold level for bit x_1	R_1	1.5
Threshold level for bit x_2	R_2	1.75
Power Splitting Factor	ρ	0.25
Time Switching Factor	τ	0.35

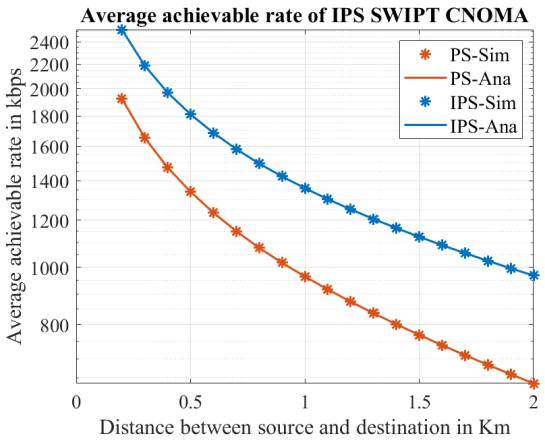

Fig. 4. Average achievable rate vs Distance for IPS-SWIPT CNOMA, (based on Eqs. (14) and (19).

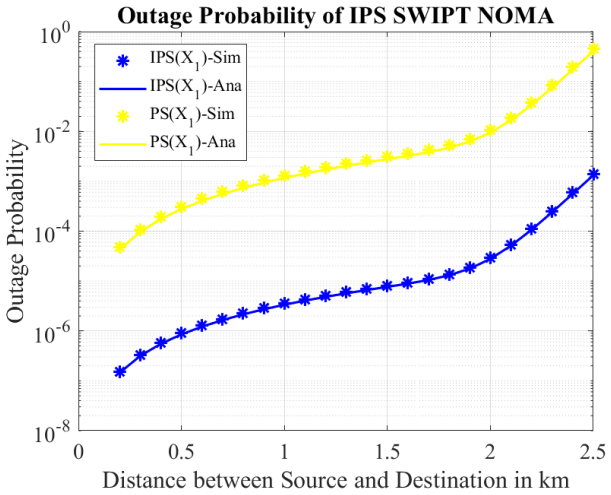

Fig. 5. Outage probability vs Distance for IPS-SWIPT CNOMA, (based on Eqs. (20) and (22).

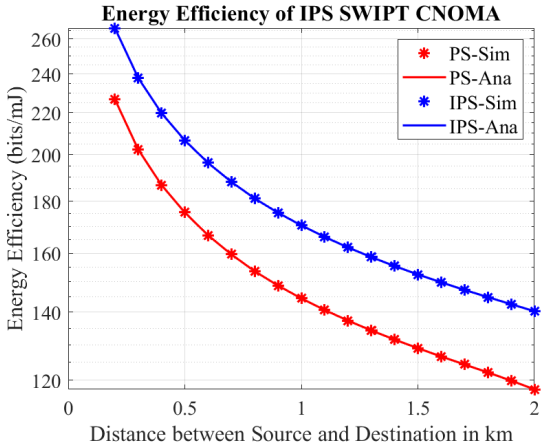

Fig. 6. Energy efficiency vs Distance for IPS-SWIPT CNOMA, (based on Eq. (23).

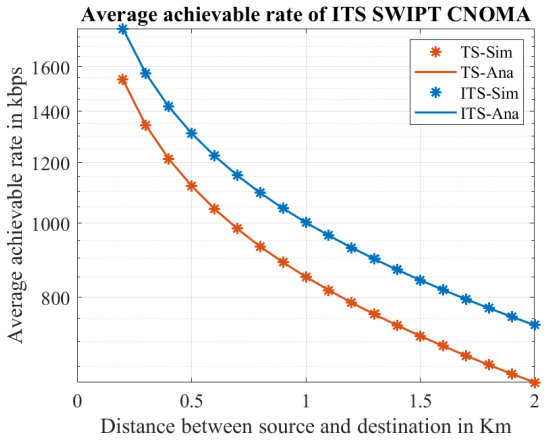

Fig. 7. Average achievable rate vs Distance for ITS-SWIPT CNOMA, (based on Eqs. (28) and (29).

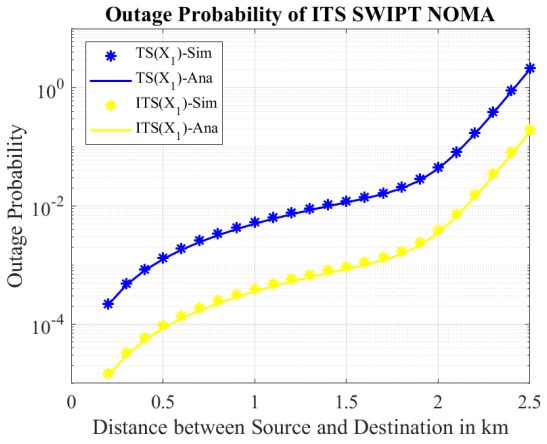

Fig. 8. Outage probability vs Distance for ITS-SWIPT CNOMA, (based on modified Eqs. (20) and (22).

across all distances compared to the conventional TS-SWIPT CNOMA.

Fig. 9 presents the energy efficiency vs distance for the ITS-SWIPT scheme. It can be observed from the results that the proposed ITS-SWIPT NOMA scheme leads to significant improvement in the energy efficiency compared to the conventional TS-SWIPT CNOMA. The simulations consider a maximum distance of 4 km and a depth of 1 km, reflecting practical UASN deployment, and for longer ranges the usable bandwidth and harvested energy decrease, which can be addressed by employing multi-hop NOMA-based architectures with SWIPT relays to extend coverage. The proposed IPS and ITS schemes require only minimal hardware changes, as bandwidth allocation is adapted based on node distance without the need for additional components.

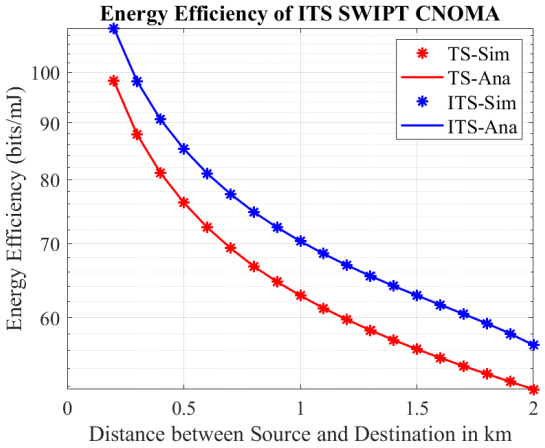

Fig. 9. Energy efficiency vs Distance for ITS-SWIPT CNOMA, (based on Eq. (23).

VI. Conclusion

In this research work, we have proposed IPS-SWIPT and ITS-SWIPT schemes for CNOMA that make use of the distance-dependent bandwidth of the underwater channel to harvest additional energy, which can significantly enhance the performance of conventional PS-SWIPT and TS-SWIPT schemes in UASNs. We have derived accurate analytical expressions for average achievable rate, energy efficiency, and outage probability for the proposed schemes by considering the underwater specific characteristics. From the analytical results, it is evident that the average achievable rate, energy efficiency, and outage probability performances are significantly improved with the proposed schemes, which exploit the additional bandwidth available to the underwater near user for harvesting energy. The analytical results are also validated with extensive Monte Carlo simulation.

References

[1] I. F. Akyildiz, D. Pompili, and T. Melodia, "Underwater acoustic sensor networks: research challenges," *Ad Hoc Networks*, vol. 3, no. 3, pp. 257–279, 2005. DOI: 10.1016/j.adhoc.2005.01.003. [Online]. Available: http://www.sciencedirect.com/science/article/pii/S1570870505000168.

[2] K. Saeed, W. Khalil, A. S. Al-Shamayleh, S. Ahmed, A. Akhunzada, S. Z. Alharthi, and A. Gani, "A comprehensive analysis of security-based schemes in underwater wireless sensor networks," *Sustainability*, vol. 15, no. 9, p. 7198, 2023. DOI: 10.3390/su15097198.

[3] A. Al Guqhaiman, O. Akanbi, A. Aljaedi, and C. E. Chow, "A survey on MAC protocol approaches for underwater wireless sensor networks," *IEEE Sensors Journal*, vol. 21, no. 3, pp. 3916–3932, 2020. DOI: 10.1109/JSEN.2020.3024995.

[4] V. Goutham and V. Harigovindan, "Full-duplex cooperative relaying with NOMA for the performance enhancement of underwater acoustic sensor networks," *Engineering Science and Technology, an International Journal*, vol. 24, no. 6, pp. 1396–1407, 2021. DOI: 10.1016/j.jestch.2021.03.008.

[5] H. H. Zuberi, S. Liu, M. Bilal, A. Alharbi, A. Jaffar, S. A. H. Mohsan, A. Miyajan, and M. A. Khan, "Deep-neural-network-based receiver design for downlink non-orthogonal multiple-access underwater acoustic communication," *Journal of Marine Science and Engineering*, vol. 11, no. 11, p. 2184, 2023. DOI: 10.3390/jmse11112184.

[6] E. A. Makled, A. Yadav, O. A. Dobre, and R. D. Haynes, "Hierarchical full-duplex underwater acoustic network: A NOMA approach," in *OCEANS 2018 MTS/IEEE Charleston*, IEEE, 2018, pp. 1–6. DOI: 10.1109/OCEANS.2018.8604904.

[7] B. Makki, K. Chitti, A. Behravan, and M.-S. Alouini, "A survey of NOMA: Current status and open research challenges," *IEEE Open Journal of the Communications Society*, vol. 1, pp. 179–189, 2020. DOI: 10.1109/OJCOMS.2020.2969899.

[8] M. Zeng, W. Hao, O. A. Dobre, and Z. Ding, "Cooperative NOMA: State of the art, key techniques, and open challenges," *IEEE Network*, vol. 34, no. 5, pp. 205–211, 2020. DOI: 10.1109/MNET.011.1900601.

[9] G. V. Goutham and V. P. Harigovindan, "NOMA Based Cooperative Relaying Strategy for Underwater Acoustic Sensor Networks Under Imperfect SIC and Imperfect CSI: A Comprehensive Analysis," *IEEE Access*, vol. 9, pp. 32857–32872, 2021. DOI: 10.1109/ACCESS.2021.3060784.

[10] J. Y. Pyun, Y. H. Kim, and K. K. Park, "Design of piezoelectric acoustic transducers for underwater applications," *Sensors*, vol. 23, no. 4, p. 1821, 2023. DOI: 10.3390/s23041821.

[11] S. Bagchi and M. Behera, "Microbial fuel cells: A sustainable technology for pollutant removal and power generation," *Bioelectrochemical Interface Engineering*, pp. 91–116, 2019. DOI: 10.1002/9781119611103.ch6.

[12] B. S. Srujana, P. Mathews, V P. Harigovindan, et al., "Multisource energy harvesting system for underwater wireless sensor networks," *Procedia Computer Science*, vol. 46, pp. 1041–1048, 2015. DOI: 10.1016/j.procs.2015.01.015.

[13] A. Khan, M. Imran, A. Alharbi, E. M. Mohamed, and M. M. Fouda, "Energy harvesting in underwater acoustic wireless sensor networks: Design, taxonomy, applications, challenges and future directions," *IEEE Access*, vol. 10, pp. 134606–134622, 2022. DOI: 10.1109/ACCESS.2022.3230600.

[14] Q. Xia, Y. Chen, C. Yang, B. Chen, G. Muhammad, and X. Ma, "Maximum efficiency point tracking for an ocean thermal energy harvesting system," *International Journal of Energy Research*, vol. 44, no. 4, pp. 2693–2703, 2020. DOI: 10.1002/er.5055.

[15] J. I. de Oliveira Filho, A. Trichili, B. S. Ooi, M.-S. Alouini, and K. N. Salama, "Toward self-powered internet of underwater things devices," *IEEE Communications Magazine*, vol. 58, no. 1, pp. 68–73, 2020. DOI: 10.1109/MCOM.001.1900413.

[16] T. D. P. Perera, D. N. K. Jayakody, S. Affes, M. Chidambaranathan, and C. Yury, "Wireless-powered hybrid terrestrial and underwater cooperative communication system," in *2019 15th International Conference on Distributed Computing in Sensor Systems (DCOSS)*, IEEE, 2019, pp. 502–506. DOI: 10.1109/DCOSS.2019.00097.

[17] Y. Tang, Q. Zhou, Z. Xie, Y. Pan, G. Ji, and X. Lü, "Research on multipath performance of acoustic spread spectrum signals based on artificial multipath experiments in an anechoic chamber," *Applied Acoustics*, vol. 218, p. 109893, 2024. DOI: 10.1016/j.apacoust.2024.109893.

[18] M. Stojanovic, "On the relationship between capacity and distance in an underwater acoustic communication channel," *ACM SIGMOBILE Mobile Computing and Communications Review*, vol. 11, no. 4, pp. 34–43, 2007. DOI: 10.1145/1327452.1327457.

[19] D. E. Lucani, M. Stojanovic, and M. Médard, "On the relationship between transmission power and capacity of an underwater acoustic communication channel," in *OCEANS 2008-MTS/IEEE Kobe Techno-Ocean*, IEEE, 2008, pp. 1–6. DOI: 10.1109/OCEANSKOBE.2008.4531073.

[20] E. M. Sozer, M. Stojanovic, and J. G. Proakis, "Underwater acoustic networks," *IEEE Journal of Oceanic Engineering*, vol. 25, no. 1, pp. 72–83, 2000. DOI: 10.1109/48.820738.

[21] J. Singh, R. Kaur, and D. Singh, "Energy harvesting in wireless sensor networks: A taxonomic survey," *International Journal of Energy Research*, vol. 45, no. 11, pp. 15861–15885, 2021. DOI: 10.1002/er.5816.

[22] H. Li, Z. D. Deng, Y. Yuan, and T. J. Carlson, "Design parameters of a miniaturized piezoelectric underwater acoustic transmitter," *Sensors*, vol. 12, no. 7, pp. 9098–9109, 2012. DOI: 10.3390/s120709098.

[23] A. Alzahrani, "High-voltage soil-based microbial fuel cells," in *2020 IEEE Texas Power and Energy Conference (TPEC)*, IEEE, 2020, pp. 1–6. DOI: 10.1109/TPEC48276.2020.9042502.

[24] T. H. Nguyen et al., "Energy outage analysis of aerial UAV-enabled SWIPT deployments," *IEEE Access*, vol. 12, pp. 27,147–27,157, 2024. DOI: 10.1109/ACCESS.2024.3366660.

[25] M. Liaqat, K. A. Noordin, T. A. Latef, K. Dimyati, T. Younas, F. Qamar, and Z. Ding, "Performance evaluation of multiple relay SWIPT-enabled cooperative NOMA network in the presence of interference," *Wireless Networks*, pp. 1–14, 2024. DOI: 10.1007/s11276-024-03669-6.

[26] N. Ashraf, S. A. Sheikh, S. A. Khan, I. Shayea, and M. Jalal, "Simultaneous wireless information and power transfer with cooperative relaying for next-generation wireless networks: A review," *IEEE Access*, vol. 9, pp. 71,482–71,504, 2021. DOI: 10.1109/ACCESS.2021.3078703.

[27] H. Sarkar, S. Sharma, and S. Kundu, "Two-user cooperative NOMA with a SWIPT-enabled relay," in *5G and Beyond Wireless Networks*, CRC Press, 2024, pp. 51–64. ISBN: 9781003407836.

[28] O. Alamu, T. O. Olwal, and K. Djouani, "Sum-rate maximization for a distributed space-time block code-aided cooperative NOMA with energy harvesting," *Wireless Networks*, pp. 1–18, 2024. DOI: 10.1007/s11276-024-03757-7.

[29] S. K. Zaidi, S. F. Hasan, and X. Gui, "Time switching based relaying for coordinated transmission using NOMA," in *2018 Eleventh International Conference on Mobile Computing and Ubiquitous Network (ICMU)*, IEEE, 2018, pp. 1–5. DOI: 10.1109/ICMU.2018.00016.

[30] K. G. Omeke, M. Mollel, S. T. Shah, L. Zhang, Q. H. Abbasi, and M. A. Imran, "Towards a sustainable internet-of-underwater-things based on AUVs, SWIPT and reinforcement learning," *IEEE Internet of Things Journal*, 2023. DOI: 10.1109/JIOT.2023.3319250.

[31] H. Esmaiel, Z. A. Qasem, H. Sun, J. Qi, J. Wang, and Y. Gu, "Wireless information and power transfer for underwater acoustic time-reversed NOMA," *IET Communications*, vol. 14, no. 19, pp. 3394–3403, 2020. DOI: 10.1049/iet-com.2020.0053.

[32] A. Wibisono, M. H. Alsharif, H.-K. Song, and B. M. Lee, "A survey on underwater wireless power and data transfer system," *IEEE Access*, 2024. DOI: 10.1109/ACCESS.2024.3373791.

[33] X. Yang, Z. Wang, T. Shen, and D. Zhao, "Modulation classification of underwater communication signals based on channel estimation," *Journal of Marine Science and Engineering*, vol. 12, no. 10, p. 1877, 2024. DOI: 10.3390/jmse12101877.

[34] S. K. Gupta, R. C. S. Chauhan, and V. Kumar, "Channel modelling in underwater media: a wireless communication technique perspective," *Physica Scripta*, vol. 99, no. 11, p. 112003, 2024. DOI: 10.1088/1402-4896/ad8282.

[35] P. Casari, M. Stojanovic, and M. Zorzi, "Exploiting the bandwidth-distance relationship in underwater acoustic networks," in *OCEANS 2007*. IEEE, 2007, pp. 1–6. DOI: 10.1109/OCEANS.2007.4449255.

[36] A. Bereketli and S. Bilgen, "Remotely powered underwater acoustic sensor networks," *IEEE Sensors Journal*, vol. 12, no. 12, pp. 3467–3472, 2012. DOI: 10.1109/JSEN.2012.2210401.

[37] H. Q. Tran, C. V. Phan, and Q.-T. Vien, "Power splitting versus time switching based cooperative relaying protocols for SWIPT in NOMA systems," *Physical Communication*, vol. 41, p. 101098, 2020. DOI:10.1016/j.phycom.2020.101098.

[38] M. C. Domingo and R. Prior, "Energy analysis of routing protocols for underwater wireless sensor networks," *Computer Communications*, vol. 31, no. 6, pp. 1227–1238, 2008. DOI: 10.1016/j.comcom.2007.11.005.

[39] H. Tran, C. Phan, and Q. Vien, "Performance analysis of power-splitting relaying protocol in SWIPT based cooperative NOMA systems," *EURASIP Journal on Wireless Communications and Networking*, vol. 2021, no. 110, pp. 1–26, 2021. DOI: 10.1186/s13638-021-01981-9.

[40] V. Aswathi and A. V. Babu, "Outage and throughput analysis of full-duplex cooperative NOMA system with energy harvesting," *IEEE Transactions on Vehicular Technology*, vol. 70, no. 11, pp. 11648–11664, 2021. DOI: 10.1109/TVT.2021.3112596.

Deepa R. (Graduate Student Member, IEEE) received the B.Tech. degree in Electronics and Communication Engineering from Pondicherry university and the M.E. Degree in VLSI Design from Anna university, Chennai, India, in 2012 and 2014, respectively. She is currently working in the Ph.D. degree in Electronics and Communication Department, National Institute of Technology Puducherry, India. Her current research focuses on nonorthogonal multiple access-based underwater wireless sensor networks.

Harigovindan V. P. (Senior Member, IEEE) received the Bachelor of Technology degree in Electronics and Communication Engineering from University of Calicut, the Master of Technology degree in Digital Electronics and Communication Systems from Visvesvaraya Technological University (with first rank), and the Ph.D. degree from the National Institute of Technology Calicut, in 2013. He is currently working as Associate Professor with the Department of Electronics and Communication Engineering, and Dean (Planning and Development) at National Institute of Technology Puducherry (under the Ministry of Education, Government of India). He has more than 75 international publications to his credit. He served as the Principal Investigator for three funded projects, each from the Department of Science and Technology, Government of India, Science and Engineering Research Board and Microsoft AI for Earth. Presently he is serving as the PI of a project funded by DST - Science for Equity, Empowerment and Development, Govt. of India. He has 5 patents granted to his credit. His research interests include wireless networks, artificial intelligence, Internet of things and wireless communications.

Veerapu Goutham is presently serving as an Assistant Professor Senior Grade 1 in the Department of Communication Engineering at the School of Electronics Engineering, Vellore Institute of Technology, located in Vellore, India. He has received his undergraduate degree in Electronics and Communication Engineering from Sri Krishnadevaraya University, Anantapur and a postgraduate degree in Digital Communications from National Institute of Technology Bhopal, India. In 2022, he received his Ph.D. degree from the National Institute of Technology Puducherry. He has more than Ten International publications and one granted patent to his credit. He is the reviewer for many SCI/SCOPUS indexed international journals namely, IEEE Transactions on Vehicular Technology, IEEE Communication Letters, IEEE Internet of Things journal and more. His research interests are in the areas of Non-Orthogonal Multiple Access, 5G and Beyond Networks, Intelligent Reflecting Surfaces, Wireless Communications, and Underwater Acoustic Sensor Networks.